The correlation and determination matrices associated with the burst design of a subsea carbon-fibre-epoxy composite flow-line

The correlation and determination matrices associated with the burst design of a subsea carbon-fibre-epoxy composite flow-line

Y Xing[1], W Xu[1], V Buratti[2]

[1]Department of Mechanical and Structural Engineering and Material Science, University of Stavanger, Kjell Arholmsgate 41, 4036 Stavanger, Norway
[2]Aibel AS, Vestre Svanholmen 14, 4313 Sandnes, Norway

Corresponding author: yihan.xing@uis.no

Abstract. This paper examines the correlation and determination matrices of the burst design in a subsea carbon-fibre-epoxy composite flow-line. A case study of a 4" flow-line is investigated. The correlation and determination matrices are calculated and compared using Pearson and Spearman correlation methods. A comprehensive suite of failure modes that comprises of Maximum Stress, Tsai-Wu, Hashin and Puck failure criteria is used to quantify the burst design. The results reveal that the failure criteria are strongly correlated to each other. The applied pressure and ply thickness are moderately correlated to the failure criteria. It is observed that due to the nature of burst loads, most material failure parameters with the exception of the Tsai-Wu constant, F_{12} do not exhibit correlations with the failure criteria. Second, both Pearson and Spearman correlation methods identified the same set of major design parameters. Third, it was found that the identification of the major design parameters is not affected by the sample size. This paper provides an analysis framework to aid in the identification of the major design parameters which is the initial and crucial step of a design optimisation exercise.

1. Introduction and background

Carbon-fibre-epoxy composite (CFEC) materials consist of an epoxy matrix reinforced by carbon fibres. The principal advantage of using CFEC materials is the high strength to weight ratio; carbon fibres are characterized by a strength-to-weight ratio 50 times higher than steel. Hence, structures made from CFEC materials are typically 20 % lighter than steel and 30% to 50% stronger. However, unlike isotropic materials, CFEC materials have directional strength properties. The orthotropic property is both an advantage and a disadvantage. CFEC materials can be aligned in the strong direction optimally to achieve higher strength-to-weight ratios in the structure. However, it requires careful design to ensure that the loads transverse to the fibre directions are not overly large; this is the weak direction. Another advantage of CFEC materials is their high fatigue strength. The fatigue limit of CFEC materials is as much as 70 % of the ultimate strength compared to only 30 % in the case of steel materials. A third advantage of using CFEC materials is their corrosion resistant properties. The above-mentioned properties make CFEC flow-lines attractive in high demanding applications.

The stress analysis and strength evaluation of CEFC flowlines have been well-studied. Some studies are briefly described here. Azar et al. [1] calculated the optimum angle of filament-wound pipelines used for natural gas transmission using approximation methods. Theotokoglou [2] used finite element analyses to quantity the effect of delamination on the loss in load carrying capacity. Xia et al. [3] analysed multi-layered filament-wound composite pipes under internal pressure using a simplified elastic solution. Chouchaoui et al. [4] studied the stresses and displacements of a laminated cylindrical tube using analytical models. Guz et al. [5] analysed the stress distributions through the pipe thickness for various lay-ups when the pipe is subjected to different outer pressure loads. These papers presented some form of parametric studies. However, there has not been any published studies applying the parametric correlation method to composite flowlines to identify the major design parameters.

This paper examines the correlation and determination matrices associated with the burst design of a 4" CFEC flow-line. Four failure criteria based on different failure theories are investigated. These are the Maximum Stress, Tsai-Wu [6], Hashin [7] and Puck [8-10] failure criteria. Furthermore, two correlation methods, namely Pearson [11, 12] and Spearman [13-15] correlation are studied. The purpose is to investigate the identification of the major design parameters associated with each individual failure criterion. The identification of the major design parameters is the initial and crucial step in a design optimization exercise [16].

Nomenclature

$\rho_{P_1P_2}$	Pearson linear correlation coefficient
$cov(P_1, P_2)$	Covariance
σ_{P_1}	Standard deviation of variable P_1
σ_{P_2}	Standard deviation of variable P_2
$\rho_{P_1^2,P_2^2}$	Pearson quadratic correlation coefficient
$\rho_{rg_{P_1},rg_{P_2}}$	Spearman linear correlation coefficient
$cov(rg_{P_1}, rg_{P_2})$	Covariance of the rank variable
$\sigma_{rg_{P_1}}$	Standard deviation of the rank variable P_1
$\sigma_{rg_{P_2}}$	Standard deviation of the rank variable P_2
$\rho_{rg_{P_1}^2,rg_{P_2}^2}$	Spearman quadratic correlation coefficient
σ_A	Axial stress
σ_H	Hoop stress
σ_1	Stress in the x-direction
σ_2	Stress in the y-direction
σ_3	Stress in the z-direction
τ_{12}	Shear stress in the xy-plane
τ_{23}	Shear stress in the yz-plane
τ_{13}	Shear stress in the xz-plane
σ_{ut1}	Ultimate tensile strength in the x-direction
σ_{uc1}	Ultimate compressive strength in the x-direction
σ_{ut2}	Ultimate tensile strength in the y-direction
σ_{uc2}	Ultimate compressive strength in the y-direction
σ_{ut3}	Ultimate tensile strength in the z-direction
σ_{uc3}	Ultimate compressive strength in the z-direction
τ_{u12}	Ultimate shear strength the in the xy-plane
τ_{u13}	Ultimate shear strength the in the xz-plane
τ_{u23}	Ultimate shear strength the in the yz-plane

2. Correlation and determination matrix

The correlation matrix measures the linear correlation between the identified design input parameters and the output variables using correlation coefficients. The correlative coefficient is a number between -1 and 1. A positive value indicates that P_2 increases with P_1, while a negative value indicates that P_2 decreases with P_1. The closer the value of correlation is to +1 or -1, the stronger the correlation between the input and the output variables. The objective of using a correlation matrix is to identify the major design parameters. The following correlation methods are used in this paper:

- Pearson correlation (Ref. Section 2.1.)
- Spearman correlation (Ref. Section 2.2.)

The determination matrix measures the quadratic correlations between P_1 and P_2. It indicates how close the points are to a quadratic curve. The determination matrix provide a measure of how well future outcomes are likely to be predicted. The correlation and determination matrices can be used to reduce the number of input parameters to a selection of major parameters in the design of experiments, or to reduce the number of output variables considered in a design optimization study.

2.1. Pearson correlation

The Pearson correlation [11, 12] is a measure of the linear correlation between two variable P_1 and P_2. The Pearson correlation coefficient is defined as:

$$\rho_{P_1P_2} = \frac{cov(P_1, P_2)}{\sigma_{P_1}\sigma_{P_2}} \tag{1}$$

Equation (1) is used in the correlation matrix. For the determination matrix, i.e., quadratic correlation, the Pearson correlation coefficient is defined as:

$$\rho_{P_1{}^2,P_2{}^2} = \frac{cov\left(P_1{}^2, P_2{}^2\right)}{\sigma_{P_1{}^2}\sigma_{P_2{}^2}} \tag{2}$$

2.2. Spearman correlation

The Spearman correlation [13-15] is defined as the Pearson correlation between the rank variables. It is given as:

$$\rho_{rg_{P_1},rg_{P_2}} = \frac{cov\left(rg_{P_1}, rg_{P_2}\right)}{\sigma_{rg_{P_1}}\sigma_{rg_{P_2}}} \tag{3}$$

Similar to the Pearson correlation, Equation (3) is used in the correlation matrix. For the determination matrix, the Spearman correlation coefficient is defined as:

$$\rho_{rg_{P_1{}^2},rg_{P_2{}^2}} = \frac{cov\left(rg_{P_1{}^2}, rg_{P_2{}^2}\right)}{\sigma_{rg_{P_1{}^2}}\sigma_{rg_{P_2{}^2}}} \tag{4}$$

Note that the symbol σ in Equation (1) to (4) is used to represent standard deviations. The symbol σ is used to represent stresses in the rest of the paper.

3. Burst design of a subsea carbon-fibre-epoxy composite flow-line

3.1. Thin wall cylinder

The flow-line is a long thin wall cylinder subjected to internal pressure. Under this load condition, an element in the cylinder wall will experience two distinct stresses, axial (σ_A) and hoop stresses (σ_H) as illustrated in Figure 1.

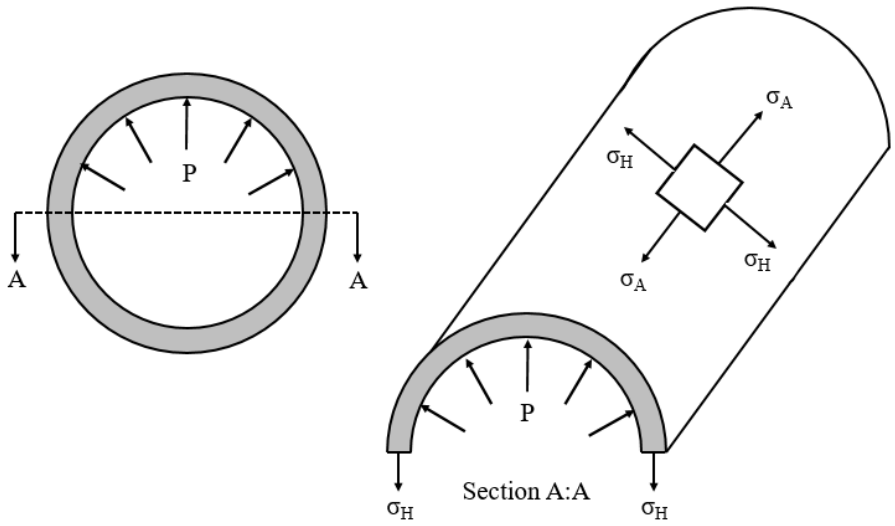

Figure 1. Stresses in a thin wall cylinder.

3.2. Classical laminate theory

The classical laminate theory (CLT) [17-19] is used in this paper. This theory extends the classical plate theory for isotropic and homogeneous materials proposed by Kirchhoff [20, 21]. The CLT assumes the following:

- There is no slip between the adjacent layers. This means that the laminate is perfectly bonded.
- Each lamina is a homogenous layer with its effective properties known and uniform throughout the lamina.
- Each lamina is in a state of plane stress
- Each lamina can be isotropic, orthotropic or inversely isotropic.
- The laminate deforms in accordance with Kirchhoff's theory. This means the normal to the mid-plane remain straight and normal to the mid-plane after deformation. In addition, the normal to the mid-plane does not change lengths.

3.3. Failure criteria

The four failure criteria listed in Table 1 are investigated in this paper. The corresponding failure theories and their failure functions are described in some details in the following sub-sections. It is mentioned that failure is defined to occur when the failure function returns a value equal or greater than 1.0.

Note that since CLT is used, the inter-laminar normal and shear stresses are zero and not computed, i.e., $\sigma_3 = \tau_{23} = \tau_{13} = 0$. However, for completeness, the generalized 3D failure criteria are presented in Section 3.3.1. to 3.3.4.

3.3.1. Maximum stress failure criterion. This failure criterion compares the ratios of the actual stresses to the failure stresses in the ply principal coordinate system. The generalized failure function is defined as:

$$f = max\left(\left|\frac{\sigma_1}{X}\right|, \left|\frac{\sigma_2}{Y}\right|, \left|\frac{\sigma_3}{Z}\right|, \left|\frac{\tau_{12}}{S}\right|, \left|\frac{\tau_{13}}{R}\right|, \left|\frac{\tau_{23}}{Q}\right|\right) \quad (5)$$

where:

$$X = \begin{cases} \sigma_{uc1}, \sigma_1 < 0 \\ \sigma_{ut1}, \sigma_1 \geq 0 \end{cases}, \quad Y = \begin{cases} \sigma_{uc2}, \sigma_2 < 0 \\ \sigma_{ut2}, \sigma_2 \geq 0 \end{cases}, \quad Z = \begin{cases} \sigma_{uc3}, \sigma_3 < 0 \\ \sigma_{ut3}, \sigma_3 \geq 0 \end{cases}$$

$$S = \tau_{u12}, \quad R = \tau_{u13}, \quad Q = \tau_{u23}$$

Table 1. Failure criteria studied.

Failure Criterion	Physical Basis	Usage Convenience	Ref. Section
Maximum Stress	Tensile behaviour of brittle material	Requires only few parameters by testing	3.3.1.
Tsai-Wu	Interactive tensor polynomial fitted to the failure behaviour of the material	Requires numerous parameters by a comprehensive testing program	3.3.2.
Hashin	Interactive criterion considering failure in fibre, transverse and delamination separately.	Requires only few parameters by testing	3.3.3.
Puck	Complex interactive criterion considering fibre and inter-fibre failures separately.	Requires numerous parameters by a comprehensive testing program	3.3.4.

3.3.2. Tsai-Wu failure criterion. The Tsai-Wu failure criterion [6] uses a quadratic failure function and is a simplification of Gol'denblat and Kapnov's generalised failure theory for anisotropic materials [22]. It is expressed as:

$$f = f_i \sigma_i + f_{ij} \sigma_i \sigma_j \tag{6}$$

where *i, j* = 1, 2, 3, 4, 5, 6. In the plane stress condition, Equation (6) reduces to:

$$f = F_{11}\sigma_1^2 + F_{22}\sigma_2^2 + F_{66}\tau_{12}^2 + 2F_{12}\sigma_1\sigma_2 + F_1\sigma_1 + F_2\sigma_2 \tag{7}$$

where $F_{11} = \frac{1}{\sigma_{ut1}\sigma_{uc1}}$, $F_{22} = \frac{1}{\sigma_{ut2}\sigma_{uc2}}$, $F_{66} = \frac{1}{S^2}$, $F_1 = \frac{1}{\sigma_{ut1}} - \frac{1}{\sigma_{uc1}}$, $F_2 = \frac{1}{\sigma_{ut2}} - \frac{1}{\sigma_{uc2}}$

and the nominal value of F_{12} is defined in Table 3.

3.3.3. Hashin failure criterion. This Hashin failure criterion [7] distinguishes the various different failure modes and model each of the modes separately. This is in contrast to the Tsai-Wu failure criterion (Ref. Section 3.3.2.) which uses a quadratic failure function that 'mixes' all the failures modes together. The Hashin failure function is defined as:

$$f = max(f_f, f_m, f_d) \tag{8}$$

where ff, fm and fd are the failure functions for failures in the fibre direction, transverse direction and delamination, respectively. For failure in the fibre direction, f_f is defined as:

$$f_f = \begin{cases} \left(\frac{\sigma_1}{\sigma_{ut1}}\right)^2 + \left(\frac{\tau_{12}}{\tau_{u12}}\right)^2 + \left(\frac{\tau_{13}}{\tau_{u13}}\right)^2, \sigma_1 \geq 0 \\ -\frac{\sigma_1}{\sigma_{uc1}}, \sigma_1 < 0 \end{cases} \tag{9}$$

For failure in the transverse direction, f_m is defined as:

$$f_m = \begin{cases} \left(\frac{\sigma_2}{\sigma_{ut2}}\right)^2 + \left(\frac{\tau_{23}}{\tau_{u23}}\right)^2 + \left(\frac{\tau_{12}}{\tau_{u12}}\right)^2 + \left(\frac{\tau_{13}}{\tau_{u13}}\right)^2, \sigma_2 \geq 0 \\ \left(\frac{\sigma_2}{2\tau_{u23}}\right)^2 + \left(\frac{\tau_{23}}{\tau_{u23}}\right)^2 + \left(\frac{\tau_{12}}{\tau_{u12}}\right)^2 + \left[\left(\frac{Y_c}{2\tau_{u23}}\right)^2 - 1\right]\frac{\sigma_2}{\sigma_{uc2}}, \sigma_2 < 0 \end{cases} \quad (10)$$

For delamination failure, f_d is defined as:

$$f_d = \begin{cases} \left(\frac{\sigma_3}{\sigma_{uc3}}\right)^2 + \left(\frac{\tau_{13}}{\tau_{u13}}\right)^2 + \left(\frac{\tau_{23}}{\tau_{u23}}\right)^2, \sigma_3 < 0 \\ \left(\frac{\sigma_3}{\sigma_{ut3}}\right)^2 + \left(\frac{\tau_{13}}{\tau_{u13}}\right)^2 + \left(\frac{\tau_{23}}{\tau_{u23}}\right)^2, \sigma_3 \geq 0 \end{cases} \quad (11)$$

3.3.4. Puck failure criteria. The Puck's action plane strength criterion is used in this paper. The criterion considers two separate failures, namely fibre failure (FF) and inter-fibre failure (IFF). For FF, the Maximum Stress criterion as defined below is used [8-10]:

$$f_{FF} = \begin{cases} \frac{\sigma_1}{\sigma_{uc1}}, \sigma_1 < 0 \\ \frac{\sigma_1}{\sigma_{ut1}}, \sigma_1 \geq 0 \end{cases} \quad (12)$$

The failure function for IFF is complex and will not be presented here. Briefly, the IFF failure function considers a 3D stress state using the definition of fracture resistances, R and slope parameters of the fracture curves, p. The Puck IFF failure function also takes into account that some fibres might already break under uniaxial loads much lower than loads which cause ultimate factors using degradation factors. Details of the IFF failure function can be found in Puck et al. [8, 9]

4. Case study

The flow-line studied is a 4" pipe with an applied pressure of 2500 psi.

4.1. Base case

The general base case properties are presented in Table 2.

Table 2. General properties of flow-line, Base case.

Property	Symbol	Value	Unit
Outer Diameter	OD	114.3	mm
Wall Thickness	WT	6	mm
Total Number of Ply	-	30	
Ply Thickness	t_{ply}	0.2	mm
Fibre orientation	-	+/- 45	°
Applied Pressure	$P_{applied}$	17.25	MPa

Table 3. Material data - ply (prepreg epoxy carbon UD)

Material Property	Symbol	Value	Unit
Elastic Modulus	E_1, E_2, E_3	121000, 8600, 8600	MPa
Shear Modulus	G_{12}, G_{23}, G_{13}	4700, 3100, 4700	MPa
Poisson's Ratio	ν_{12}, ν_{23}, ν_{13}	0.27, 0.4, 0.27	-
Tensile Strength	σ_{ut1}, σ_{ut2}, σ_{ut3}	2231, 29, 29	MPa
Compressive Strength	σ_{uc1}, σ_{uc2}, σ_{uc3}	-1082, -100, -100	MPa
Shear Strength	τ_{u12}, τ_{u23}, τ_{u13}	60, 32, 60	MPa
Tsai-Wu Constants	F_{12}, F_{23}, F_{13}	-1, -1, -1	-
Puck Constants	p_{21+}, p_{22+}, p_{21-}, p_{22-}	0.35, 0.25, 0.3, 0.25	-
Additional Puck Constants	s, M, F_{IW}	0.5, 0.5, 0.8	-

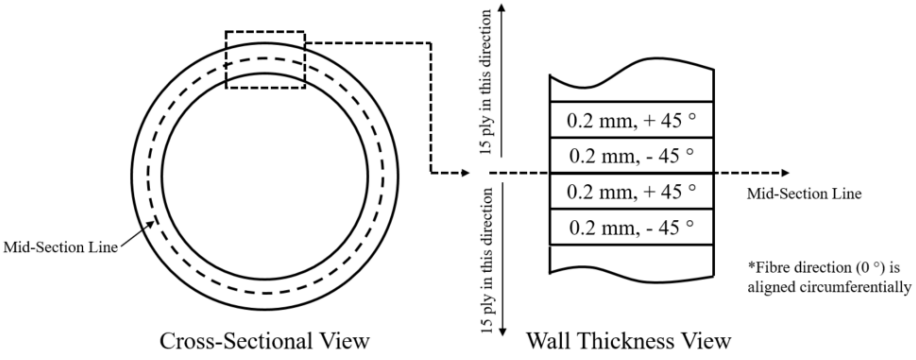

Figure 2. Stacking sequence.

The base case failure criteria values, corresponding to the base case design talked into this sub-section, are presented in Table 4. These are calculated using the finite element model presented in Section 4.2. The results are calculated using the mesh size of 10 mm as discussed in Section 4.2.2. The failure modes are mainly caused by the matrix, i.e., the material fails in shear. The Tsai-Wu failure criterion does not distinguish failure modes. One can also notice the large difference in failure values calculated using Maximum Stress failure criterion vs. the rest of the criteria. This is because Maximum Stress failure criterion does not consider the strength contribution from the fibre when evaluating matrix failure. In this particular case, the strength contribution from the fibres would be significant as they are aligned 45° to the direction of hoop stress and therefore help to share some of the load away from the matrix.

Table 4. Base case failure criteria values.

	Maximum Stress	Tsai-Wu	Hashin	Puck
Failure Criterion Value	0.642	0.905	0.899	0.934
Failure Mode	τ_{u12} exceeded	-	Matrix failure	Matrix tension failure

4.2. Finite element model

A 2 000 mm section of the flow-line is modeled. This is considered to be sufficiently long by engineering judgement in order to avoid end effects due to loads and boundary conditions in the finite element model. The results are obtained at the middle part of the section, i.e., at the 1 000 mm point. ANSYS R17.0 is used for the finite element modelling.

4.2.1. Loads and boundary conditions. The loads and boundary conditions applied on the model are illustrated in Figure 3. Pressure (Load A) is applied in the interior of the flow-line. Fixed support (Load B) is applied on the right edge of the flow-line. An end cap force (Load C) due to the internal pressure is applied on the left edge of the flow-line.

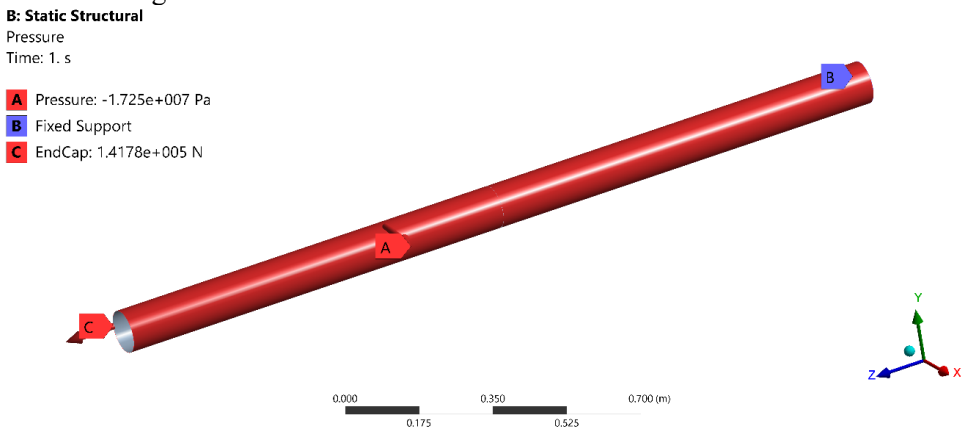

Figure 3. Loads and boundary conditions

4.2.2. Mesh refinement study. The cases studied and the corresponding results obtained for the mesh refinement study are presented in Table 5 and Figure 4 respectively. The element used is the 4-node SHELL181 element [23]. The results show that a 10 mm element size is sufficient to produce converged solutions for the four failure criteria investigated in this paper. The mesh details used in this paper are presented in Figure 5.

Table 5. Cases studied for mesh refinement study

Element Size (mm)	No. of Elements	No. of Nodes
30	888	900
20	900	1 552
15	2 904	2 926
10	6 386	6 400
5	24 896	24 960

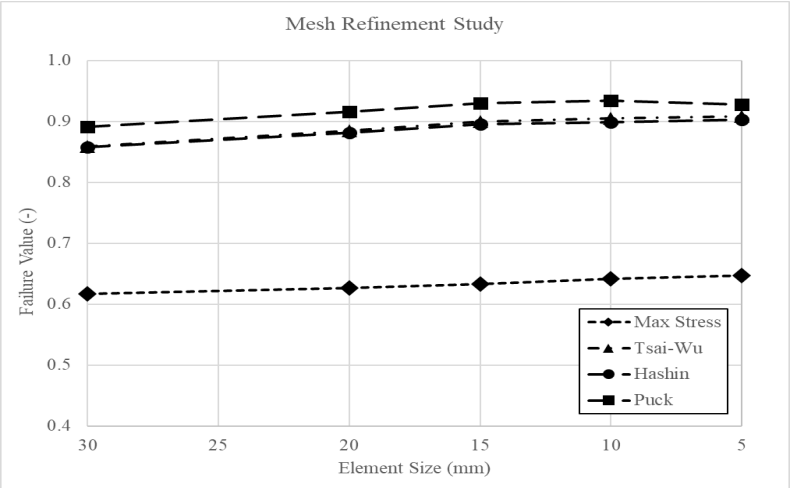

Figure 4. Results of mesh refinement study.

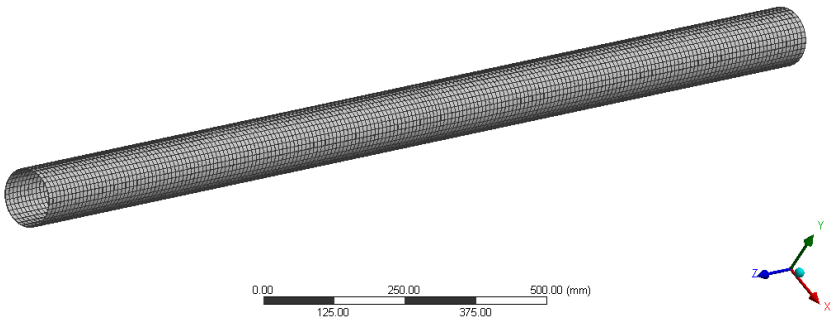

Figure 5. Mesh details, 10 mm element size, 6 386 SHELL181 elements with 6 400 nodes.

4.2.3. Example result plots. An example plot of the maximum stress failure is presented in Figure 6. The maximum value generated by the failure function in the middle of the 2 000 mm flow-line is extracted and used in this paper.

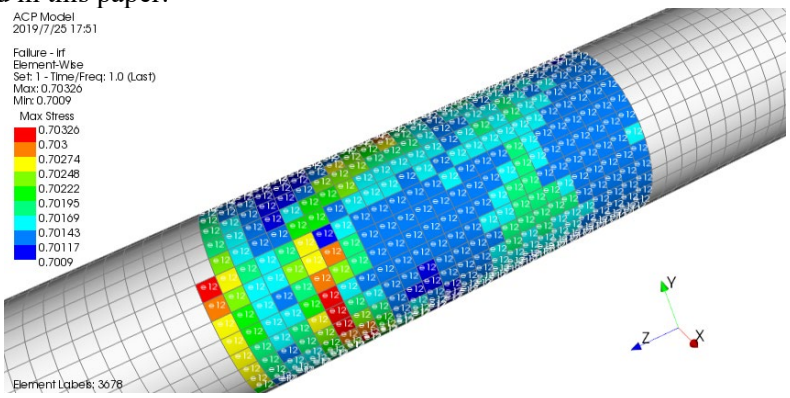

Figure 6. Example plot of maximum stress failure.

5. Results and discussions

5.1. Correlation and determination matrices

The correlation and determination matrices are presented in Figure 7 and Figure 8, respectively. The matrices are calculated using Spearman correlation method and a sample size of 200. Notice that the correlation matrix is symmetrical. However, the determination matrix is not symmetrical. This is because $Cov(P_1^2,P_2^2) \neq Cov(P_2^2,P_1^2)$ The matrix calculated using the Pearson correlation identified the same set of major design parameters and therefore not presented here. The comparison of Pearson and Spearman correlation methods is presented in Section 5.2. The observations made are presented in the following sub-sections.

5.1.1. Strong correlations between failure criteria. The failure criteria have strong linear and quadratic correlations with one and other. The values of these correlations are all above 0.8. This is intuitive, an increase in the failure value calculated from one failure criterion will imply that the failure values calculated from other failure criteria would also increase. A detailed investigation into the correlation values presented in Table 6 and Table 7 revealed that the correlation is stronger between the Tsai-Wu, Hashin and Puck criteria. The Maximum Stress criterion is not as correlated, particularly for the quadratic correlations. This could be explained that Tsai-Wu, Hashin and Puck criteria are non-linear criteria while the Maximum Stress criterion is a linear criterion. In addition, Tsai-Wu and Hashin have failure functions of a quadratic nature.

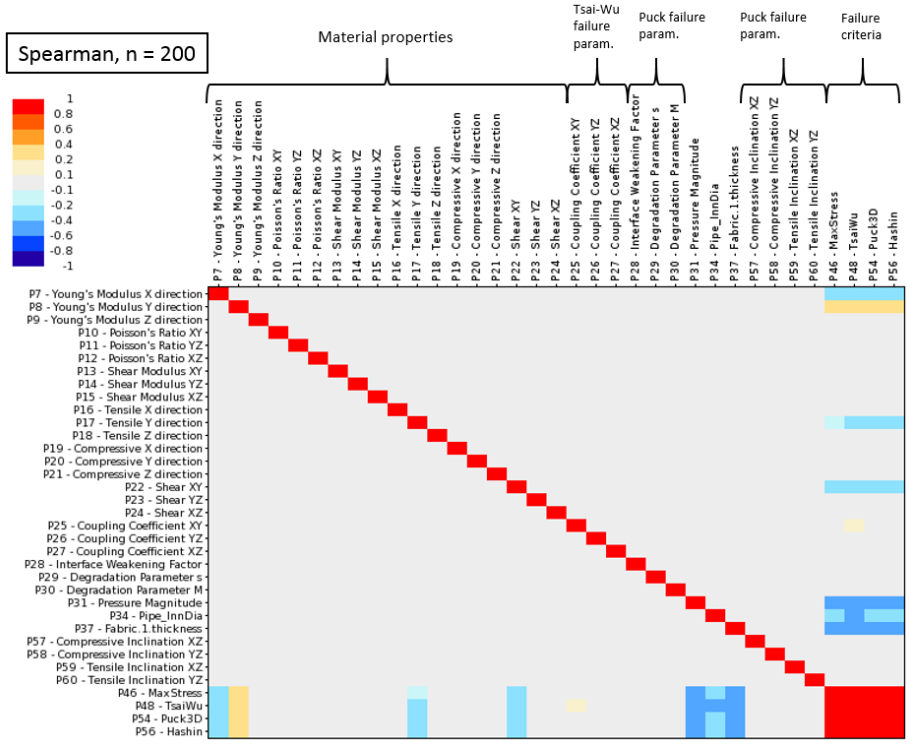

Figure 7. Correlation matrix, Spearman correlation, n = 200.

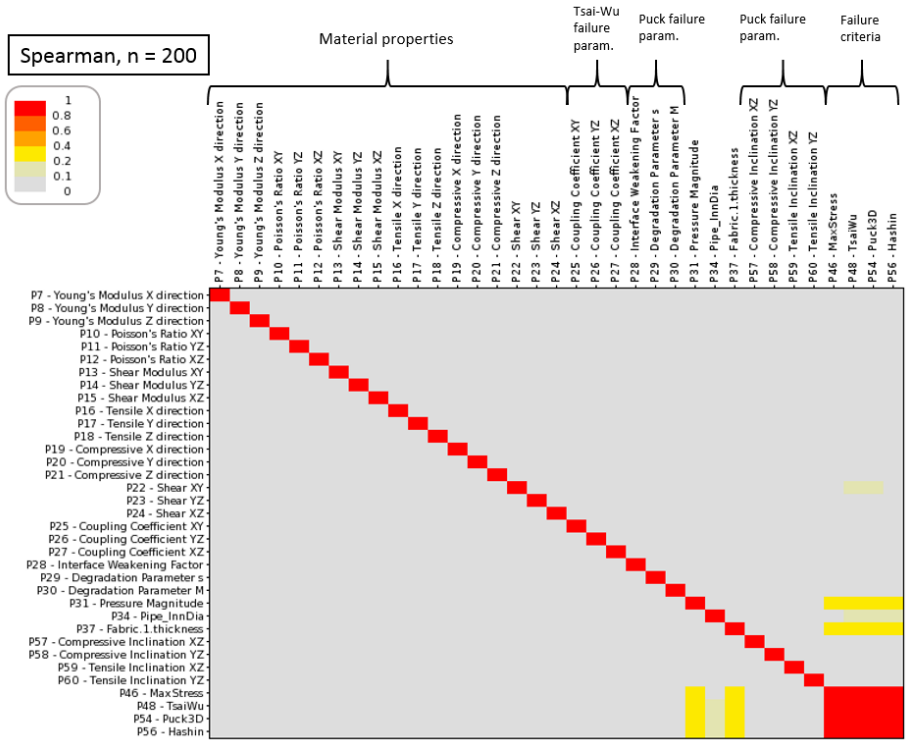

Figure 8. Determination matrix, Spearman correlation, n = 200.

Table 6. Spearman linear correlation, n = 200, failure criteria

	Maximum Stress	Tsai-Wu	Hashin	Puck
Maximum Stress	1.00	0.90	0.91	0.91
Tsai-Wu	0.96	1.00	0.96	0.97
Hashin	0.91	0.96	1.00	0.99
Puck	0.91	0.97	0.99	1.00

Table 7. Spearman quadratic correlation, n = 200, failure criteria

	Maximum Stress	Tsai-Wu	Hashin	Puck
Maximum Stress	1.00	0.81	0.83	0.84
Tsai-Wu	0.81	1.00	0.94	0.96
Hashin	0.82	0.94	1.00	0.98
Puck	0.84	0.96	0.98	1.00

5.1.2. Moderate correlations between applied pressure & ply thickness and failure criteria. The applied pressure, $P_{applied}$ and ply thickness, t_{ply} are moderately linearly correlated (0.4 to 0.6 or -0.6 to -0.4) with the failure criteria. These parameters are also slightly quadratically correlated (0.1 to 0.4 or -0.4 to -0.1). It is intuitive to understand that applied pressure and ply thickness would be naturally correlated with the failure criteria. The counter-intuitive thing is that the correlation is not strong. It can be natural to think that since hoop stress is directly proportional to the applied pressure and inversely proportional to wall thickness, therefore the correlation must be very strong. The moderate correlations can be understood by taking a closer examination at the correlation scatter diagram of Puck failure criteria vs. applied pressure and ply thickness as presented in Figure 9. Note the applied pressure (horizontal axis) is plotted in decreasing values, i.e., the right side of the horizontal axis denotes smaller values of applied pressure. From Figure 9, it is clear that the scatter is quite large; this is due to the fact that failure of the flow-line is not just fully dependent on the values of applied pressure and/or ply thickness but a result of many design parameters at play.

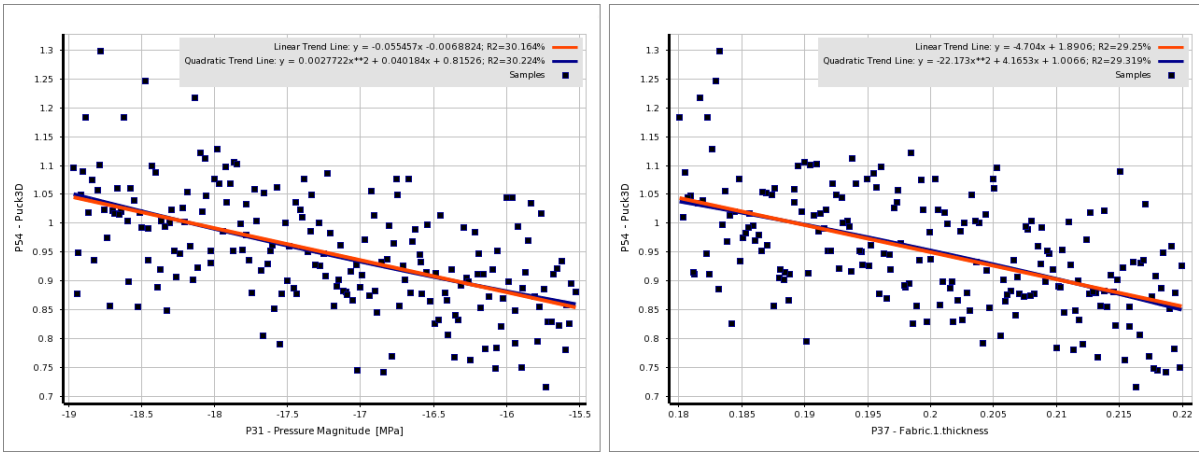

Figure 9. Correlation scatter diagram, Puck failure criterion vs. applied pressure and ply thickness, Spearman correlation, n = 200.

5.1.3. Other parameters with slight correlation with failure criteria. The parameters that have slight linear correlations (0.1 to 0.4 or -0.4 to -0.1) with the failure criteria are elastic moduli, E_1, E_2, tensile strength, σ_{ut1}, shear strength, τ_{u12} and outer diameter, OD. In addition, Tsai-Wu constant, $F_{12,}$ has a slight correlation with the Tsai-Wu failure criterion. The other parameters that have slight quadratic correlations (0.1 to 0.4 or -0.4 to -0.1) with the failure criteria are shear strength, τ_{u12} and outer diameter, OD. The slight correlations of tensile strength σ_{ut1} and shear strength τ_{u12} can be surprising to the reader. However, this can be understood by examining their correlation scatter diagrams. Figure 10 presents the correlation scatter diagrams of Maximum Stress criterion vs tensile strength σ_{ut1} and shear strength τ_{u12}. It becomes clear why these two design parameters are only slightly correlated to the Maximum Stress criterion. As previously mentioned in Section 5.1.2. , the failure of the flow-line is not just dependent ontensile strength σ_{ut1} and shear strength τ_{u12} , but it is a result of many design parameters at play.

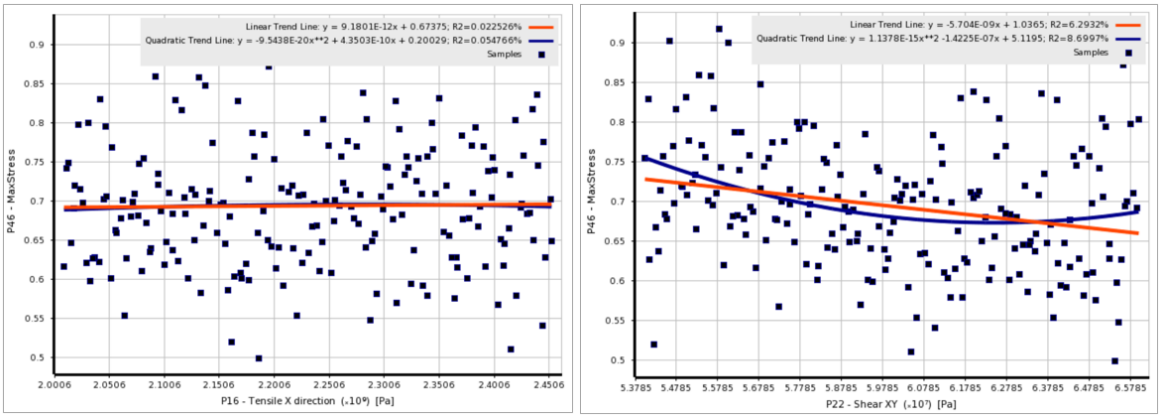

Figure 10. Correlation scatter diagram, maximum stress criterion vs. tensile strength σ_{ut1} and shear strength τ_{u12}, Spearman correlation, n = 200

5.1.4. Most material-related failure parameters insignificantly correlated with failure criteria. Most material-related failure parameters with the exception of Tsai-Wu constant, $F_{12,}$ do not exhibit correlation (below |0.1|) to the failure criteria. This is due to the nature of the current loading considered which predominantly result in membrane stress along the pipe walls. This causes the load to be predominantly in the fibre direction. The failure parameters in the failure criteria, i.e., Tsai-Wu constants and all Puck constants considered are primarily defined to model transverse, bending and/or inter-laminar loading. It is expected that these failure parameters would play a more important role in the failure criteria when more complex loadings are considered.

5.2. Pearson vs. Spearman

Both Pearson and Spearman correlation methods identified the same set of major design parameters as presented in Figure 11 and Figure 12.

5.3. Effect of sample size

In general, the larger the sample size, the more likely design parameters with lower values of correlation get highlighted in the correlation and determination matrices. However, the governing design parameters, i.e., parameters with higher values of correlation would still be highlighted on the matrices. This is highlighted by the example presented in Figure 13 where the Spearman correlation matrix from n = 50 is compared against n = 200. It is observed that the darker coloured squares, i.e., high correlation values are practically the same for n = 50 and n = 200. The difference is in the lighter coloured squares, i.e., low correlation values. For practical engineering purposes, a sample size of 100 seemed to be sufficient in this paper.

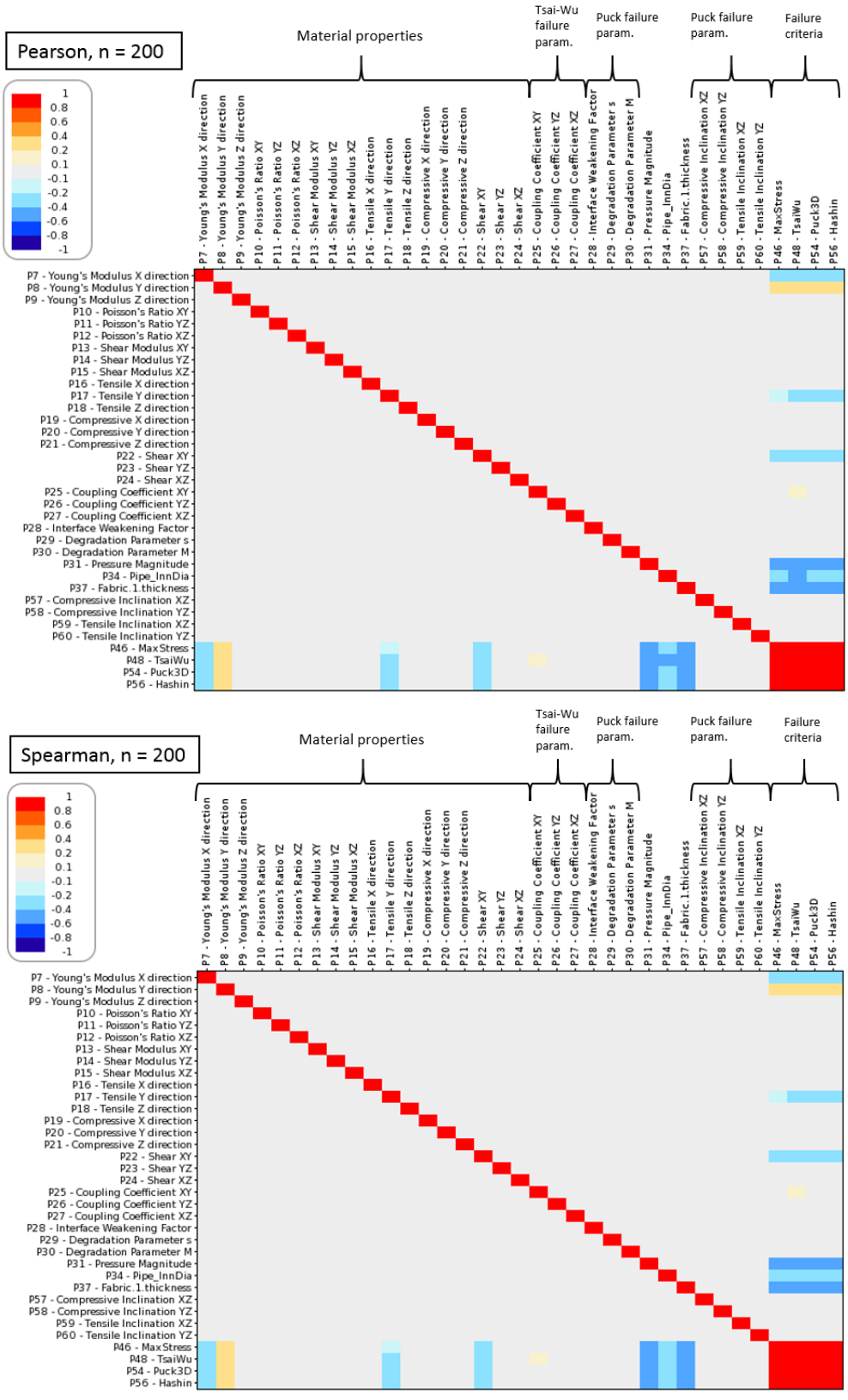

Figure 11. Comparison of linear correlation matrices, Pearson vs. Spearman.

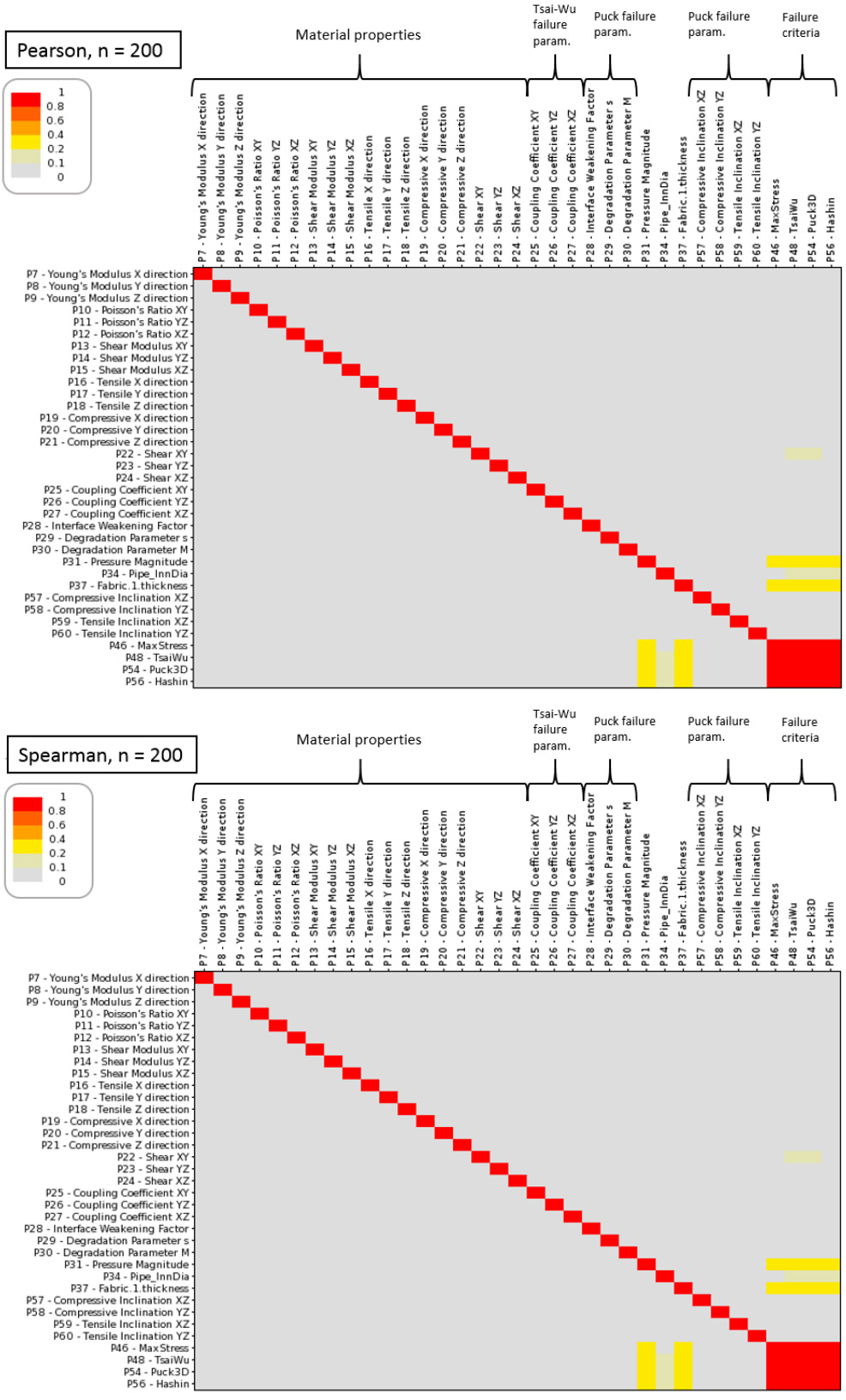

Figure 12. Comparison of quadratic correlation matrices, Pearson vs. Spearman

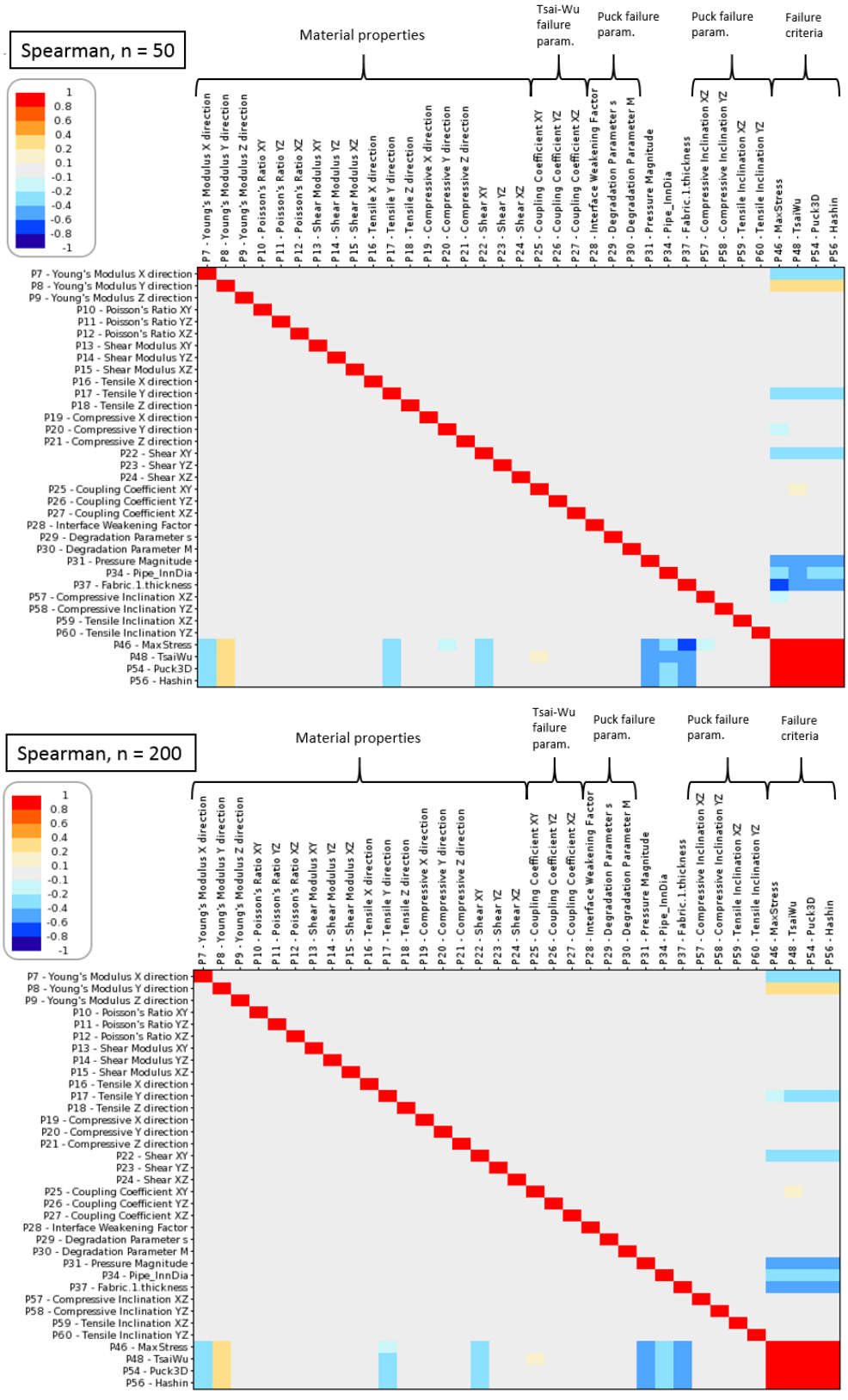

Figure 13. Comparison of correlation matrices, Spearman correlation, n = 50 vs. n = 200.

6. Conclusions

The following conclusions are made:

- Strong linear and quadratic correlations are observed between the failure criteria.
- Moderate linear and slight quadratic correlations are observed between applied pressure & ply thickness and the failure criteria.
- Most material failure parameters with the exception of Tsai-Wu constant, $F_{12,}$ are not strongly correlated to the failure criteria. This can be explained by the fact that the loads experienced by the flow-line are pre-dominantly in the fibre direction.
- Both Pearson and Spearman correlation methods identified the same set of major design parameters for the correlation matrix.
- The effect of sample size is not profoundly significant to the results. There were no large differences found in using sample sizes of 50 vs. 100 vs. 200. For practical engineering purpose a sample size of 100 is recommended.

7. Future work

There are plans to extend the study to include (i) external tension/compression forces and bending moments, (ii) response surface development and optimisation and (iii) six-sigma analysis. Furthermore, additional failure modes such as fatigue and collapse can be studied in future work. Other design scenarios such as pipeline global buckling and installation can also be investigated. The objective is to provide a framework for the design optimisation of flow-lines when non-traditional materials such as CFEC are used.

References

[1] Reza Khoshravan Azar M, Emami Satellou A A, Shishesaz M and Salavati B 2013 Calculating the optimum angle of filament-wound pipes in natural gas transmission pipelines using approximation methods, *J. Pressure Vessel Technol*. **135**(2), 021702.
[2] Theotokoglou E E 2006 Behaviour of thick composite tubes considering of delamination, *Theor. Appl. Fract. Mech.* **46**(3), 276-85.
[3] Xia M, Takayanagi H and Kemmochi K 2001 Analysis of multi-layered filament-wound composite pipes under internal pressure, *Compos. Struct.* **53**(4), 483-91.
[4] Chouchaoui C S and Ochoa O O 1999 Similitude study for a laminated cylindrical tube under tensile, torsion, bending, internal and external pressure. Part I: governing equations, *Compos. Struct.* **44**(4), 221-29.
[5] Guz I A, Menshykova M and Paik J K 2017 Thick-walled composite tubes for offshore applications: an example of stress and failure analysis for filament-wound multi-layered pipes, *Ships and Offshore Structures.* **12**(3), 304-22.
[6] Tsai S W and Wu E M 1971 A general theory of strength for anisotropic materials, *J. Compos. Mater.* **5**(1), 58-80.
[7] Hashin Z 1980 Failure criteria for unidirectional fiber composites, *J. Appl. Mech*. **47**(2), 329.
[8] Puck A 1996 Festigkeitsanalyse von faser-matrix-laminaten. (Carl Hanser).
[9] Puck A 1998 Failure analysis of FRP laminates by means of physically based phenomenological models, *Compos. Sci. Technol*. **58**(7), 1045-67.
[10] Puck A 2002 Schürmann H. Failure analysis of FRP laminates by means of physically based phenomenological models, *Compos. Sci. Technol*. **62**(12-13), 1633-62.
[11] Pearson K 1920 Notes on the history of correlation, *Biometrika.* **13**(1), 25-45.
[12] Pearson K 1986 Mathematical contributions to the theory of evolution. III. Regression, Heredity, and Panmixia, *Philos. Trans. R. Soc. London, Ser. A, Containing Papers of a Mathematical or Physical Character.* **187**, 253-318.
[13] Spearman C E 1904 The proof and measurement of association between two things, *Am. J. Psychol.* **15**, 72-101.

[14] Spearman C E 1904 General intelligence, objectively determined and measured, *Am. J. Psychol.* **15**, 201-93.
[15] Spearman C E 1910 Correlation calculated from faculty data, *Br. J. Psychol*, 1904-1920. **3**(3), 271-95.
[16] Vanderplaats G N 2007 Multidiscipline design optimization (Colorado Springs)
[17] Nettles A T 1994 Basic mechanics of laminated composite plates. (Marshall Space Flight Center, NASA).
[18] Palantera M 1998 ESAComp 4.1 - theoretical background of ESAComp analyses.
[19] Jones R M 1975 Mechanics of composite material (Hemisphere).
[20] Kirchhoff G 1850 Über das gleichgewicht und die bewegung einer elastischen scheibe, *J. Reine und Angewante Mathematik* (Crelle). **40**, 51-88.
[21] Love A E H 1906 A treatise on the mathematical theory of elasticity (Cambridge).
[22] Gol'denblat II, Kopnov V A 1966 Strength of glass-reinforced plastics in the complex stress state - english translation, *Polymer Mechanics.* **1**, 54.
[23] ANSYS®. Academic research mechanical, release 17.0, help system, element reference, chapter I, SHELL181, ANSYS, Inc.